

# Performance Evaluation of Purely Mechanical Wireless In-Mould Sensor for Injection Moulding

Florian Müller, Christian Kukla, Thomas Lucyshyn, Clemens Holzer

**Abstract**—In this paper, the influencing parameters of a novel purely mechanical wireless in-mould injection moulding sensor were investigated. The sensor is capable of detecting the melt front at predefined locations inside the mould. The sensor comprises a movable pin which acts as the sensor element generating structure-borne sound triggered by the passing melt front. Due to the sensor design, melt pressure is the driving force. For pressure level measurement during pin movement a pressure transducer located at the same position as the movable pin. By deriving a mathematical model for the mechanical movement, dominant process parameters could be investigated towards their impact on the melt front detection characteristic. It was found that the sensor is not affected by the investigated parameters enabling it for reliable melt front detection. In addition, it could be proved that the novel sensor is in comparable range to conventional melt front detection sensors.

**Index Terms**—Injection Moulding, In-Mould Sensor, Structure-Borne Sound, Wireless Sensor

## I. INTRODUCTION

INJECTION moulding is a highly dynamic process designed to produce high-precision technical parts in mass production scale. To assure reproducibility of the injection-moulded parts, control strategies are necessary to compensate changing process conditions. Wang et al. [1] propose a three-level categorized system for injection moulding process control. The first level deals with controlling of machinery related parameters such as barrel temperature, injection rate or clamping force. These parameters can in general be controlled independently and accurately using closed loop control strategies [1]–[3]. Industry often selects this approach for part quality control 'hoping that the found process parameter set is good enough' [4].

The second level comprises process parameters, e.g. melt temperature, melt pressure or melt front advancement. This set of parameters is closely related to the part quality. Finally, level three parameters involve the most complex parameters, the quality related parameters, such as part weight, shrinkage and warpage or optical defects of the part [1]. Of course, it would be great to directly control these parameters to ensure constant quality; however, the lack of appropriate in-mould sensors to detect quality parameters is undeniable. This lack is recognized by researches for some time now and they insist to lay a strong focus on developing in-mould sensor concepts for quality control measurements [2], [4].

Nowadays, two types of in-mould sensors are mainly used to

monitor or control the injection moulding process: cavity wall temperature sensors and cavity pressure sensors [5]. Cavity wall temperature sensors are only in some cases used for temperature sensing while more often for melt front detection. Due to the low mass and small sensor head diameter, the sensors have short response times of around<sup>1</sup> 10 ms and are suitable for melt front detection [6], [7]. Melt front detection is also possible using cavity pressure sensors which is reported in [8]–[10] for instance.

In injection moulding there are several cases in which it is of special interest to know the transient position of the melt front. One of these points is at the end of the filling phase where the machine has to switch-over from a volumetric controlled to a pressure controlled filling condition [11]. This point is at around 98% volumetric cavity filling [10]. In a machine centric approach this point is whether located using the current ram position or using a timer. However, when process parameters change, e.g. viscosity change due to batch-to-batch variation, the melt front propagation varies to the cycles before. Consequently, in a machine centric approach the switch-over point is not the same to the shots before resulting in varying part quality. In several publications it is emphasized to utilize in-mould sensors for precise switch-over point detection since it is crucial for having constant accurate part quality [6], [12], [13].

One of the major disadvantages of all common available in-mould sensors is the necessity of wiring for energizing as well as data transmission. A mould needs complex structural modification to enable implementation of wire ducts [14]. Moreover, sometimes it is not even possible to find sufficient space for implementation of in-mould sensors since cooling channels, sliders as well as ejector pins have a higher priority in the design process because they are crucial in defining part quality and mould functionality. In addition, wires introduce significant disadvantages to the overall lifetime of a mould due to their sensitive nature, e.g. rupturing. Furthermore, if a sensor fails during processing most parts of the mould have to be disassembled to enable the exchanging of the sensor.

In recent years a movement towards wireless in-mould sensors has been initiated. Since the year 2002 a research group in the US develops and investigates a self energized wireless in-mould sensor [15]. The sensor uses the pressure inside the melt to generate electricity for sensing process parameters such as pressure and temperature. The measurement data is transmitted to the outside surface of the mould using ultrasonic structure-borne sound [16]–[18]. With this design

<sup>1</sup>For a cavity wall temperature sensor with a head diameter of 1 mm.

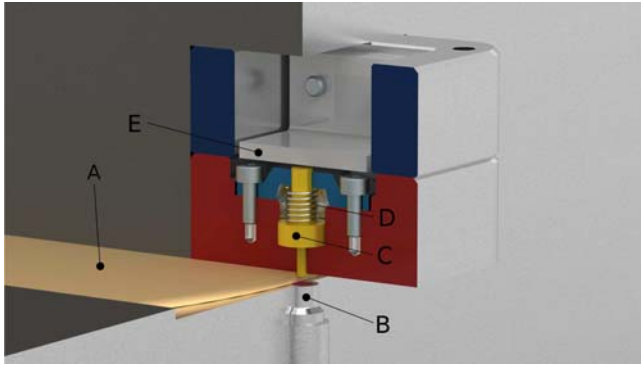


Fig. 1. Rendered section view of the implemented acoustic actuator inside the mould. The melt front *A* influxes the cavity and overflows the pressure transducer *B* which is positioned at the direct opposite cavity side of the acoustic actuator. The acoustic actuator comprises a movable pin *C*, a supporting spring *D*, ensuring initial position of the pin at the beginning of an injection moulding cycle, and a resonant structure *E*.

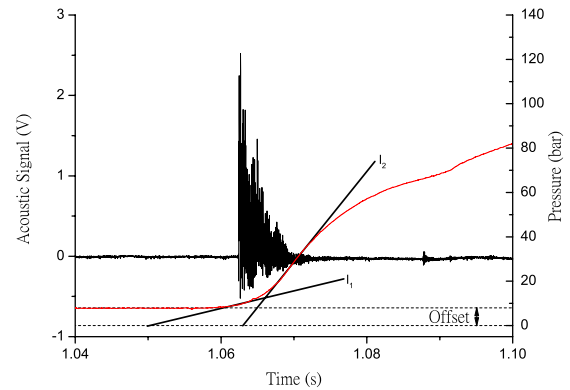


Fig. 2. Pressure measurement with an injection rate of  $60 \text{ cm}^3\text{s}^{-1}$ . Red line indicates pressure level and black line indicates acoustic signal. The pressure history was approximated using two straight lines  $l_1$  and  $l_2$  for estimation of pressure influence on pin movement.

only minor structural modifications are necessary for sensor implementation. Furthermore, this system enables placing a plurality of transmitters into a mould by only mounting one receiver at the outside surface of the mould making it more efficient.

Recently, a novel purely mechanical wireless in-mould sensor was presented [19] which is capable of detecting the melt front at predetermined locations. Thereby, a purely mechanical actuator is implemented in the mould comprising a movable pin (Fig. 1 *C*) a supporting spring *D* and a resonant structure *E*. The movable pin towers with a height  $d$  into the cavity at the beginning of an injection moulding cycle. As soon as the melt front reaches the pin it gets accelerated towards the resonant structure until it impacts on it. At this point the pin lines up precisely with the cavity wall leading to a conventional ejector pin mark on the part surface. Due to the impact, the resonant structure oscillates with its resonant frequency which can be detected by an outside surface mounted accelerometer. If multiple acoustic actuators are implemented in the mould separation can be achieved by designing differently shaped resonant structures, all having different resonant frequencies. For the automatic detection of the resonant frequencies in the recorded acoustic signal a novel algorithm was introduced making use of linear algebra and polynomial basis function sets [20].

It should be mentioned that the acoustic actuator in this design is only used during investigation of the acoustic-emission sensor. The main goal of the research is to use conventional ejector pins for resonant structure excitement. In this manner, ejector pins would gain an additional functionality for detecting the melt front without losing their conventional functionality of demoulding parts [20].

In this paper, a performance evaluation of the novel system is given investigating several influencing parameters, such as melt pressure respective viscosity, spring rate of the actuator as well as the mass of the movable pin. These parameters are the essential parameters defining the overall mechanical performance of the acoustic-emission sensor.

## II. EXPERIMENTS AND RESULTS

The measurements were performed on an Arburg 470A-1000 injection moulding machine using an easy flowing polypropylene (PP) C7069-100A from Dow Chemical Company, Switzerland. The polymer has a zero shear viscosity of  $100 \text{ Pa}\cdot\text{s}$  at a temperature of  $240^\circ\text{C}$ . The used mould was especially built for investigating and developing the acoustic-emission sensor. For the pressure measurements, a 6157 pressure transducer from Kistler, Switzerland, with a head diameter of 4 mm was incorporated. For the recording of the structure-borne sound, a 352A60 from PCB Piezotronics Inc., USA, with a sensitivity of  $10.16 \text{ mV/g}$  and a frequency range ( $\pm 3\text{dB}$ ) from 5 up to 60000 Hz was utilized. The data acquisition was done using a data acquisition toolbox (DAQ-box) USB-6366 from National Instruments, USA. The DAQ-box sampled the two independent channels, one channel for the accelerometer and the other one for the pressure transducer, using a sampling rate of  $f_s = 120 \text{ kHz}$  ( $\tau \cong 8 \mu\text{s}$ ).

### A. Pressure Measurement

The pin movement of the acoustic-emission sensor is mainly dependent on the pressure propagation inside the melt. To detect pressure levels during the pin movement, a pressure transducer was positioned at the same flow path position as the movable pin, but on the opposite cavity side. As a result, both independent measurement systems experience the same conditions enabling comparison of the systems. In Fig. 1 the measurement design is shown as a rendered section view. The melt front *A* is in-fluxing the cavity, passing both, the pressure transducer *B* as well as the movable pin *C* at the same time.

In Fig. 2 measurement results using an injection rate of  $60 \text{ cm}^3\text{s}^{-1}$  are shown. The red line indicates the pressure level having an increase around 1.06s after start of the filling phase. Almost simultaneously a large deflection is recognizable in the acoustic signal indicating the impact of

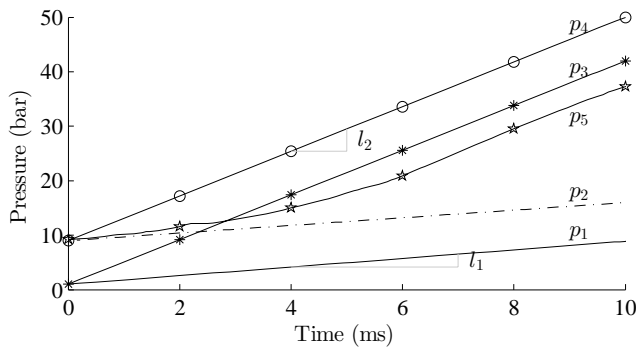


Fig. 3. Five time-dependent pressures  $p_i$  used for calculating pin movement.  $p_1$  starts at 0 bar with inclination  $l_1$  (solid line);  $p_2$  starts at 9 bar with inclination  $l_1$  (dashed dotted line);  $p_3$  starts at 0 bar with inclination  $l_2$  (solid line with asterisk marker);  $p_4$  starts at 9 bar with inclination  $l_2$  (solid line with circle marker); and  $p_5$  is the real measurement data (solid line with five pointed star marker). The inclinations  $l_1$  and  $l_2$  were obtained by measurement data shown in Fig. 2.

the movable pin<sup>2</sup>.

It is known that pressure transducer may deliver incorrect results as long as the sensor head is not fully overflowed by melt and is exposed to asymmetric loading. Having an injection rate of  $60 \text{ cm}^3 \text{ s}^{-1}$  and a cavity width of 20 mm and 2 mm in height in the region of sensor implementation, around 2.6 ms is needed to overflow the sensor with a head diameter of 4 mm. However, the time needed to fully overflow the sensor head is mainly the time at which pin movement happens. To consider this probable inaccuracy during pressure measurement two linear approximations  $l_1$  and  $l_2$  with different inclination of the pressure trend from Fig. 2 are introduced. Thereby line  $l_1$  covers the recorded pressure level at the beginning of pin movement. Line  $l_2$  has a steeper inclination and is introduced to cover possible inaccurate pressure data. The pressure trends  $p$ , which are introduced next, are then plugged into a mathematical model used for calculating time dependent pin movement. As a result, the influence of different acting pressure levels on the pin movement can be estimated.

The first line  $l_1$  approximates the pressure trend at the beginning of overflowing the sensor head having an inclination of  $\Delta p / \Delta t = 0.7 \text{ bar} / 1 \text{ ms}$ . The second line is in the region of higher pressure increase having an inclination of  $\Delta p / \Delta t = 4.0 \text{ bar} / 1 \text{ ms}$ .

In Fig. 2 it can be observed that the pressure level is not at 1 bar level at the moment before the melt front reaches the sensor head but an offset level of around 9 bar is obvious. This happens although the measurement system is reset at the beginning of an injection moulding cycle. Yet, the exact reason for this offset can not be given at this point but either a problem with venting of the cavity or a problem with implementation of the sensor could be the reason. To cover these uncertainties, four different pressure histories are set

<sup>2</sup>In Müller [19] it was shown that this deflection originates only from the acoustic actuator and not from any other random source. To proof this, the acoustic actuator was replaced by a blanked insert. As a result, at the temporal point where the deflection had occurred before now only noise is detected. Consequently, the deflection before was a result of the implemented acoustic actuator.

up,  $p_1$  starting at pressure level 1 bar having inclination  $l_1$ ,  $p_2$  starting at the measured level 9 bar having an inclination of  $l_1$ , too. Pressure level  $p_3$  is again starting at pressure level 0 bar and  $p_4$  starts from 9 bar. Both pressure levels have inclination  $l_2$ . Finally a fifth pressure level  $p_5$  is set up using the real measurement data. The five pressures are shown time-dependent in Fig. 3 and are plugged into the mathematical model of the pin movement to investigate the dependence of the measurement system on this influencing parameter.

### B. Mathematical Description of Pin Movement

For sensor performance estimation it is interesting to know the time needed for the pin to go from the initial position to the distance  $d$  at which it impacts the resonant structure. This time can be seen as a delay time in the melt front detection and should be as low as possible. The structure-borne sound is propagating with a velocity of  $5000 \text{ ms}^{-1}$  in the metal mass of the mould resulting in nearly no transmission delay [21]. Additionally, a delay due to digital signal processing occurs. The sum of all the delays is the overall delay of the acoustic-emission sensor<sup>3</sup>. For the acoustic-emission sensor two different distances for pin movement were tested,  $d_1 = 0.1 \text{ mm}$  and  $d_2 = 0.5 \text{ mm}$ . The shorter distance  $d_1$  results in quicker response time but the greater distance  $d_2$  results in a better signal to noise ratio since impact energy is larger. Since the pin movement is not directly measurable, as a result of the mould setup, a mathematical approach is formulated. Thereby, some assumptions and simplifications have to be made to enable solving the governing equation, i.e. frictionless movement, neglect of gravitation or venting conditions of the cavity<sup>4</sup>. At first, the system of interest has to be described. In case of the acoustic-emission sensor an unidirectional movable pin, accelerated by an increasing melt pressure acting on a constant area, as well as a spring, have to be described. The differential equation for this system can be written as,

$$m\ddot{x}(t) = F(t) - kx(t), \quad (1)$$

where  $m$  is the mass of the pin,  $k$  denotes the spring rate,  $x(t)$  the time dependent position as well as its second temporal derivative  $\ddot{x}(t)$ , the time dependent acceleration.  $F(t)$  holds the time dependent force acting on the pin area. Since the pin has a circular shape the force acting on the pin's surface as a result of melt pressure can be calculated as,

$$F(t) = p(t)A = p(t)r^2\pi, \quad (2)$$

with  $r = 1 \text{ mm}$  as the pin radius. In Bronštejn [22] a solution for such a type of differential equation can be found leading to,

$$x(t) = \frac{F(t) - F(t) \cos\left(t\sqrt{\frac{k}{m}}\right)}{k} \quad (3)$$

<sup>3</sup>In the data sheets of the manufacturer of in-mould sensors the response time of the sensors is always stated without signal processing.

<sup>4</sup>Venting will have a major influence on the acoustic-emission sensor. However, overall performance will be an interaction between spring ratio, friction, venting and process parameters.

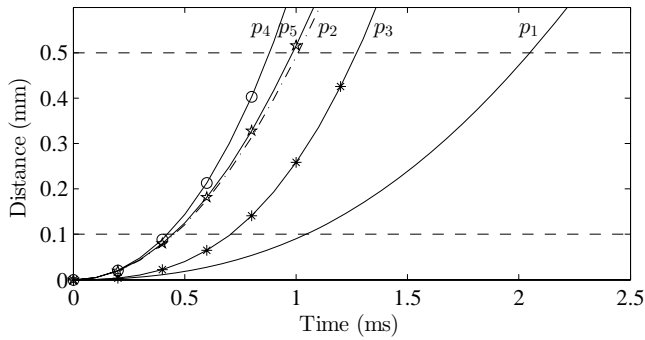


Fig. 4. Time-dependent calculated pin movement using Eq. 3 for five different pressure histories.  $p_1$  starts at 0 bar with inclination  $l_1$  (solid line);  $p_2$  starts at 9 bar with inclination  $l_1$  (dashed dotted line);  $p_3$  starts at 0 bar with inclination  $l_2$  (solid line with asterisk marker);  $p_4$  starts at 9 bar with inclination  $l_2$  (solid line with circle marker); and  $p_5$  is the real measurement data (solid line with five pointed star marker). Pin mass and spring rate were set constant.

With Eq. 3 the influence of the force  $F(t)$  and thus the pressure, the spring ratio  $k$  and the pin mass  $m$  can be investigated.

### C. Pressure Influence Investigation

The five different pressure levels  $p_i$  can now be plugged into Eq. 3 resulting in a time dependent pin movement. The used spring (D-068A-17) has a spring rate  $k_1 = 1.179 \text{ N/mm}$  and is from Gutekunst + Co.KG Federnfabriken, Germany. The mass of the movable pin is  $m = 3 \cdot 10^{-3} \text{ kg}$ . In Fig. 4 the pin movement for the five different pressure setups  $p_i$  is shown as a function of time.

Starting with the lowest pressure  $p_1$  (solid line), the pin needs about 1.0ms to overcome a distance of 0.1 mm and 1.85 ms for the distance of 0.5 mm. By using the pressure history with the higher offset level,  $p_2$  (dashed dotted line), the time needed to reach both distances reduce by approximately 50 % each. For the higher pressure gradient  $l_2$  less time is needed when comparing each pressure history with its identical offset pressure level, i.e.  $p_1$  and  $p_2$ . When using the recorded values from the pressure measurement ( $p_5$  star marked line) a pin movement similar to  $p_3$  is obtained. The pin needs about 1 ms until impact for a distance of 0.5 mm.

Although a difference in the response time of over 100 % was estimated between pressure level  $p_1$  and  $p_4$  for the distance of  $d_2 = 0.5 \text{ mm}$ , the absolute time difference is in a range of just over 1 ms. Conventional in-mould sensing technology for melt front detection is in similar range concerning response characteristic, e.g. cavity wall temperature sensors [23].

From the obtained results it gets clear that the response time of the sensor varies in a small window although widely different pressure data were used. As a result it is safe to state that sensor response characteristic is robust against pressure variation.

In addition, the injection rate of the moulding machine was widely varied to influence the melt pressure level. For the pressure rates already used, three additional injection rates were set,  $15 \text{ cm}^3\text{s}^{-1}$  resulting in pressure  $p_6$ ,  $30 \text{ cm}^3\text{s}^{-1}$  resulting in pressure  $p_7$  and  $120 \text{ cm}^3\text{s}^{-1}$  resulting in pressure

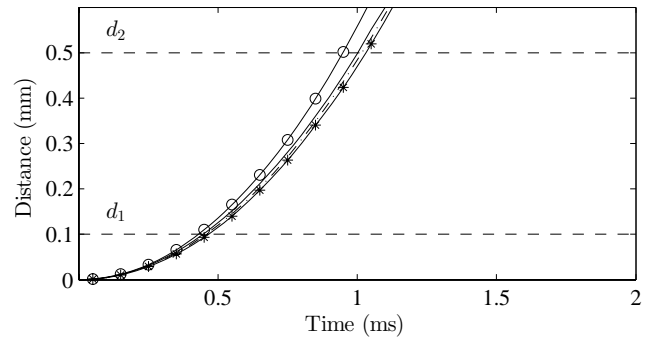


Fig. 5. Pin movement as function of time while having four widely different injection rates.  $15 \text{ cm}^3\text{s}^{-1}$  displayed as solid line;  $30 \text{ cm}^3\text{s}^{-1}$  as dashed dotted line;  $60 \text{ cm}^3\text{s}^{-1}$  as solid line with asterisk marker and  $120 \text{ cm}^3\text{s}^{-1}$  as solid line with circle marker.

trend  $p_8$ . The obtained pressure results were plugged into Eq. 3 receiving the pin movement shown in Fig. 5. Surprisingly the pin movement is calculated very similar for all four different injection rates which one would not expect.

An explanation for this behaviour can be found when the pressure curves of the different injection rates are investigated. In Fig. 6 the recorded pressure trends of the different injection rates are shown in a short milli-second time window. As it can be seen the pressure levels  $p_5 - p_6$  are very similar for all measurements up to 3 ms and follow an expected trend from then on. Only pressure level  $p_8$  starts rising earlier. However, the pin movement happens in the time before 3 ms.

An influencing factor which has to be mentioned here is the data set cut-out. For the low injection rates it is quite hard to find the exact moment of pressure increase in the data set. This fact, however, is not of significant relevance since by shifting the data cut-out to later moments would only result in better response time characteristic. Hence, the shown pin movement is a worst case assumption.

The variation of the pressure level can also be seen as varying the melt viscosity. In Pahl et al. [24] the viscosity of a Newtonian fluid is described as,

$$\eta_N = \frac{H^3 B \Delta p}{12 \dot{V} L}, \quad (4)$$

with  $L$  as the length of the chamber,  $H$  and  $B$  are the height and width (remember  $L \gg B \gg H$ ),  $\dot{V}$  the volume flow rate and  $\eta_N$  the Newtonian viscosity. When holding the geometry of the chamber and also the injection rate constant a variation in the pressure drop is similar to having a material with different viscosity. The used PP has a low viscosity in comparison to typical used thermoplastics for injection moulding. Consequently, for typical high-viscosity polymers the already observed response time characteristics in Fig. 4 will be even better, since the pressure propagation inside the melt will have a higher inclination resulting in a higher acceleration of the movable pin. This fact supports the usage of the acoustic-emission sensor for a wide variety of polymers.

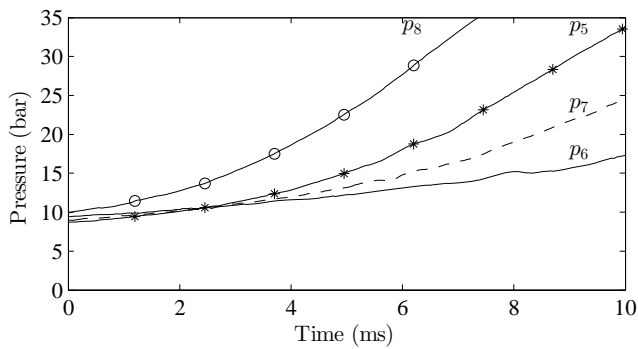


Fig. 6. Melt pressure recorded with four different injection rates plotted as function of time.  $15 \text{ cm}^3\text{s}^{-1}$  displayed as solid line referred to  $p_6$ ;  $30 \text{ cm}^3\text{s}^{-1}$  as dashed dotted line referred to  $p_7$ ;  $60 \text{ cm}^3\text{s}^{-1}$  as solid line with asterisk marker referred to the already introduced  $p_5$  and  $120 \text{ cm}^3\text{s}^{-1}$  as solid line with circle marker referred to  $p_8$ .

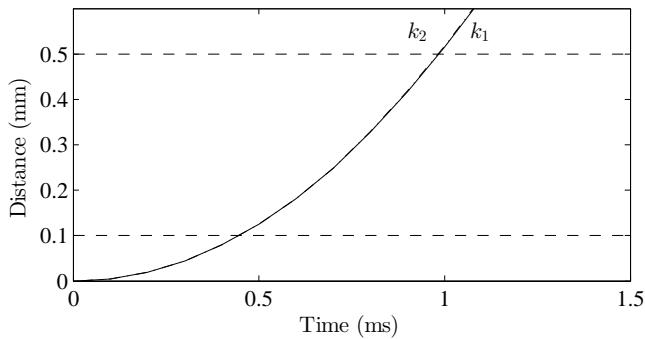


Fig. 7. Time-dependent calculated pin movement for two different spring types (solid line  $k_1 = 1.179 \text{ N/mm}$  and dashed line  $k_2 = 1.013 \text{ N/mm}$ ).

#### D. Spring Rate Influence Investigation

Another important part of the acoustic actuator is the supporting spring. The spring pushes with a certain force against the movable pin ensuring a correct initial position at each injection moulding cycle. The force of the spring is acting against the movement direction of the pin consuming some of the kinetic energy. As a result, it has to be considered in the performance evaluation. A spring is described by its spring rate which is the proportional factor between force and compression/relaxation.

In the housing of the acoustic actuator only a certain amount of space is available limiting the range of possible springs. The two used springs<sup>5</sup> have a spring rate  $k_1 = 1.179 \text{ N/mm}$  and  $k_2 = 1.013 \text{ N/mm}$ . Plugging both spring rates into Eq. 3 results in the pin movement shown in Fig. 7. As it can be observed there is nearly no change in the pin movement characteristic using either one. For the measurement the mass of the pin was set to  $m = 3 \cdot 10^{-3} \text{ kg}$  and the pressure history  $p_5$  at injection rate  $60 \text{ cm}^3\text{s}^{-1}$  was used.

#### E. Pin Mass Influence Investigation

Finally, the influence of the pin mass was investigated. This parameter is of special interest with regard to using

<sup>5</sup>The second spring (VD-068A-17) is from Gutekunst + Co.KG Federnfabriken, Germany, too.

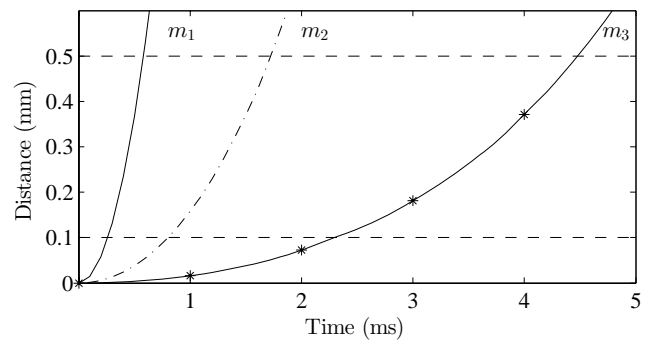


Fig. 8. Time-dependent pin movement for three differently assumed masses,  $m_1$  the smallest mass shown as solid line,  $m_2$  shown as dashed dotted line and  $m_3$  as solid line with asterisk marker.

ejector pins as the movable pins exciting the resonant structure. The currently used pin has a mass of  $m = 3 \cdot 10^{-3} \text{ kg}$ . However, this mass is very low and as it was shown that around  $0.5 - 2 \text{ ms}$  is needed to pass the distance  $d$ . To investigate the influence of mass three different masses of various orders of magnitude are incorporated in Eq. 3, i.e.  $m_1 = 10^{-3} \text{ kg}$ ,  $m_2 = 10^{-2} \text{ kg}$  and  $m_3 = 10^{-1} \text{ kg}$ . In Fig. 8 the results are shown. As it can be seen, with increasing pin mass the time to overcome the distance  $d$  is overproportional increasing. For the highest pin mass  $m_3$ ,  $4.5 \text{ ms}$  is needed to overcome distance  $d_2 = 0.5 \text{ mm}$ . However, the response time values are still in comparable range with those of commonly used cavity wall temperature sensors with a bigger sensor head diameter, e.g. Priamus 4007B which has a head diameter of  $1.0 \text{ mm}$  and has a stated response time of  $4 \text{ up to } 10 \text{ ms}$  [25]. Nevertheless, pin mass has the highest influence of all the investigated parameters and with respect to designing ejector pins with the ability to excite the resonant structure, mass reduction should be considered.

### III. CONCLUSION

In this paper influencing performance parameters for a novel purely mechanical wireless in-mould sensor for injection moulding were investigated. The actuator comprising a movable pin is driven by the pressure inside the melt front which was measured using a pressure transducer. It was observed that measuring the present pressure level is difficult since the whole pin movement happens below  $5 \text{ ms}$  at low pressure levels. However, the measured pressure is a underestimation of the current level leading to even better response characteristic than estimated. Since the variation of pressure propagation can also be seen as a change in viscosity the acoustic-emission sensor concept is functional for a wide variety of thermoplastics.

It was found that the mass of the movable pin has the most significant impact on the overall sensor characteristic. Especially in reference to adapt ejector pins to overtake the function of the movable pin, mass becomes a critical factor. Consequently, mass optimization has to be performed when implementing the acoustic-emission sensor concept on ejector pins which is the main target of the research. However,

even with the highest established mass the time needed to overcome the distance  $d_2$  is in the range of the response time of conventional cavity wall temperature sensors.

The last investigated parameter was the spring rate. It was found that exchanging the spring with other available ones does not affect the sensor characteristic in a significant way. In conclusion it can be stated that the sensor performance of the acoustic-emission sensor is at least similar to the conventional available in-mould sensing technology, but having the benefit of not needing wires inside the mould. Furthermore, the response characteristic of the acoustic-emission sensor is hardly affected by varying influencing parameters (excluding pin mass) making it suitable for the usage in the injection moulding process for melt front detection.

#### ACKNOWLEDGMENT

The research work was supported by the project PolyRegion which is founded by the European Territorial Cooperation SI-AT.

#### REFERENCES

- [1] K. K. Wang, J. Zhou, and Y. Sakurai, "An Integrated Adaptive Control for Injection Molding," in *Proceedings of ANTEC 1999*, New York City, 1999.
- [2] Z. Chen and L.-S. Turng, "A review of current developments in process and quality control for injection molding," *Advances in Polymer Technology*, vol. 24, no. 3, pp. 165–182, 2005.
- [3] J. Giboz, T. Copponnex, and P. Mélé, "Microinjection molding of thermoplastic polymers: a review," *Journal of Micromechanics and Microengineering*, vol. 17, no. 6, pp. 96–109, 2007.
- [4] D. O. Kazmer, S. P. Johnston, R. Gao, and Z. Fan, "Feasibility Analysis of an In-mold Multivariate Sensor," *International Polymer Processing The Journal of the Polymer Processing Society*, vol. XXVI, no. 01, pp. 63–72, 2011.
- [5] D. O. Kazmer, *Plastics manufacturing systems engineering: [a systems approach]*. München: Hanser Verlag, 2009.
- [6] D. O. Kazmer, S. Velusamy, S. Westerdale, S. Johnston, and R. Gao, "A comparison of seven filling to packing switchover methods for injection molding," *Polymer Engineering and Science*, vol. 50, no. 10, pp. 2031–2043, 2010.
- [7] C. Bader, "Das kleine Einmaleins der Werkzeug-Sensorik," *Kunststoffe International*, no. 6, pp. 114–117, 2006.
- [8] T. Hirano, "Automated Switchover in Injection Molding," *Journal of the Japan Society of Polymer Processing*, vol. 9, no. 11, p. 843, 1997.
- [9] M.-S. Huang, "Cavity pressure based grey prediction of the filling-to-packing switchover point for injection molding," *Journal of Materials Processing Technology*, vol. 183, no. 2-3, pp. 419–424, 2007.
- [10] B. Sheth, C. M. Barry, N. R. Scott, R. D. Higdon, and B. Davison, "Improved part quality using cavity pressure switchover," in *Proceedings of ANTEC 2001*, Dallas, 2001.
- [11] F. Johannaber and W. Michaeli, *Handbuch Spritzgießen*, 2nd ed. München: Hanser, 2004.
- [12] C. Collins, "Monitoring cavity pressure perfects injection molding," *Assembly Automation*, vol. 19, no. 3, pp. 197–202, 1999.
- [13] A. Kelly, M. Woodhead, and P. Coates, "Comparison of injection molding machine performance," *Polymer Engineering & Science*, vol. 45, no. 6, pp. 857–865, 2005.
- [14] L. Zhang, C. B. Theurer, R. Gao, and D. O. Kazmer, "Design of ultrasonic transmitters with defined frequency characteristics for wireless pressure sensing in injection molding," *IEEE Transactions on Ultrasonics Ferroelectrics and Frequency Control*, vol. 52, no. 8, pp. 1360–1371, 2005.
- [15] L. Zhang, C. B. Theurer, R. Gao, and D. O. Kazmer, "DEVELOPMENT OF A WIRELESS PRESSURE SENSOR WITH REMOTE ACOUSTIC TRANSMISSION," *Transaction North American Manufacturing Research Institute*, vol. 30, pp. 573–580, 2002.

- [16] Z. Fan, R. Gao, and D. O. Kazmer, "Design of a self-energized wireless sensor for simultaneous pressure and temperature measurement," *Advanced Intelligent Mechatronics (AIM)*, 2010 IEEE/ASME International Conference on Advanced Intelligent, Montreal, 2010.
- [17] C. Theurer, Li Zhang, D. O. Kazmer, R. Gao, and R. Jackson, "Passive charge modulation for a wireless pressure sensor," *IEEE Sensors Journal*, vol. 6, no. 1, pp. 47–54, 2006.
- [18] L. Zhang, C. B. Theurer, and R. Gao, "A SLEF-ENERGIZED SENSOR FOR WIRELESS INJECTION MOLD CAVITY PRESSURE MEASUREMENT: DESIGN AND EVALUATION," *Journal of dynamic systems, measurement, and control*, vol. 126, no. 2, pp. 309–318, 2004.
- [19] F. Muller, G. Rath, T. Lucyshyn, C. Kukla, M. Burgsteiner, and C. Holzer, "Presentation of a novel sensor based on acoustic emission in injection molding," *Journal of Applied Polymer Science*, vol. 127, no. 6, pp. 4744–4749, 2013.
- [20] F. Müller, P. O'Leary, G. Rath, M. Harker, T. Lucyshyn, and C. Holzer, "Resonant Acoustic Sensor System for the Wireless Monitoring of Injection Moulding," in *Sensornets 2013, 2nd International Conference on Sensor Networks*, Barcelona, 2013.
- [21] B. Heißing, *Fahrwerkhandbuch*. Wiesbaden: Springer Fachmedien, 2008.
- [22] I. N. Bronštejn, *Taschenbuch der Mathematik*, 19th ed. Thun and Frankfurt/Main: Deutsch, 1981.
- [23] C. Bader and S. C. Zeller, "Die Entdeckung der Schmelzefront: Sensortechnik," *Kunststoff Magazin Online*, no. 6, pp. 2–6, 2010.
- [24] M. Pahl, W. Gleissle, and H.-M. Laun, *Praktische Rheologie der Kunststoffe und Elastomere*, 4th ed. Düsseldorf: VDI-Verl., 1995.
- [25] Priamus System Technologies AG, "Datashet 4007B / 4008B," Schaffhausen and Switzerland, 2013.

**Florian Müller** is PhD student at the chair of Polymer Processing at the Montanuniversität Leoben, Austria, since 2010. He works in the field of wireless in-mould sensors for injection moulding as well as micro and nano structuring of polymer surfaces using injection moulding.

**Dr. Christian Kukla** is responsible for applied R&D and the development of new products together with companies within his expertise in injection moulding, tooling, production process and PIM.

**Ass.Prof. Thomas Lucyshyn** is Assistant Professor and head of the injection moulding group at the Chair of Polymer Processing at the Montanuniversität Leoben, Austria, with a research focus on injection moulding and simulation.

**Prof. Dr. Clemens Holzer** is head of the Chair of Polymer Processing at the Department of Polymer Engineering and Science and full professor at Montanuniversität Leoben. The main research themes are injection moulding, extrusion, compounding, simulation and determination of material data.